**Supplementary Figure 1**. Methylation pattern of wild type and mutant WNV NS5 MTases. Recombinant wild type and mutant E218A MTase domain of WNV NS5 (N-terminal 300 amino acids) were assayed for N7 and 2'O methylation. The cloning and purification of the wild type and mutant MTases were described in [1]. The N7 methylation was measured by the G*pppA-RNA➔m⁷G*pppA-RNA (the asterisk indicates that the following phosphate is ^{32}P labeled) conversion. The 2'O methylation was monitored by the m⁷G*pppA-RNA➔m⁷G*pppAm-RNA conversion. The reactions were digested with nuclease P1 to release different cap structures (G*pppA, m⁷G*pppA, and m⁷G*pppAm), which were separated on polyethyleneimine cellulose thin-layer chromatography plates. The methylation activities of the mutant are indicated with the wild type set at 100%. The details of the methylation assays were described previously [1].
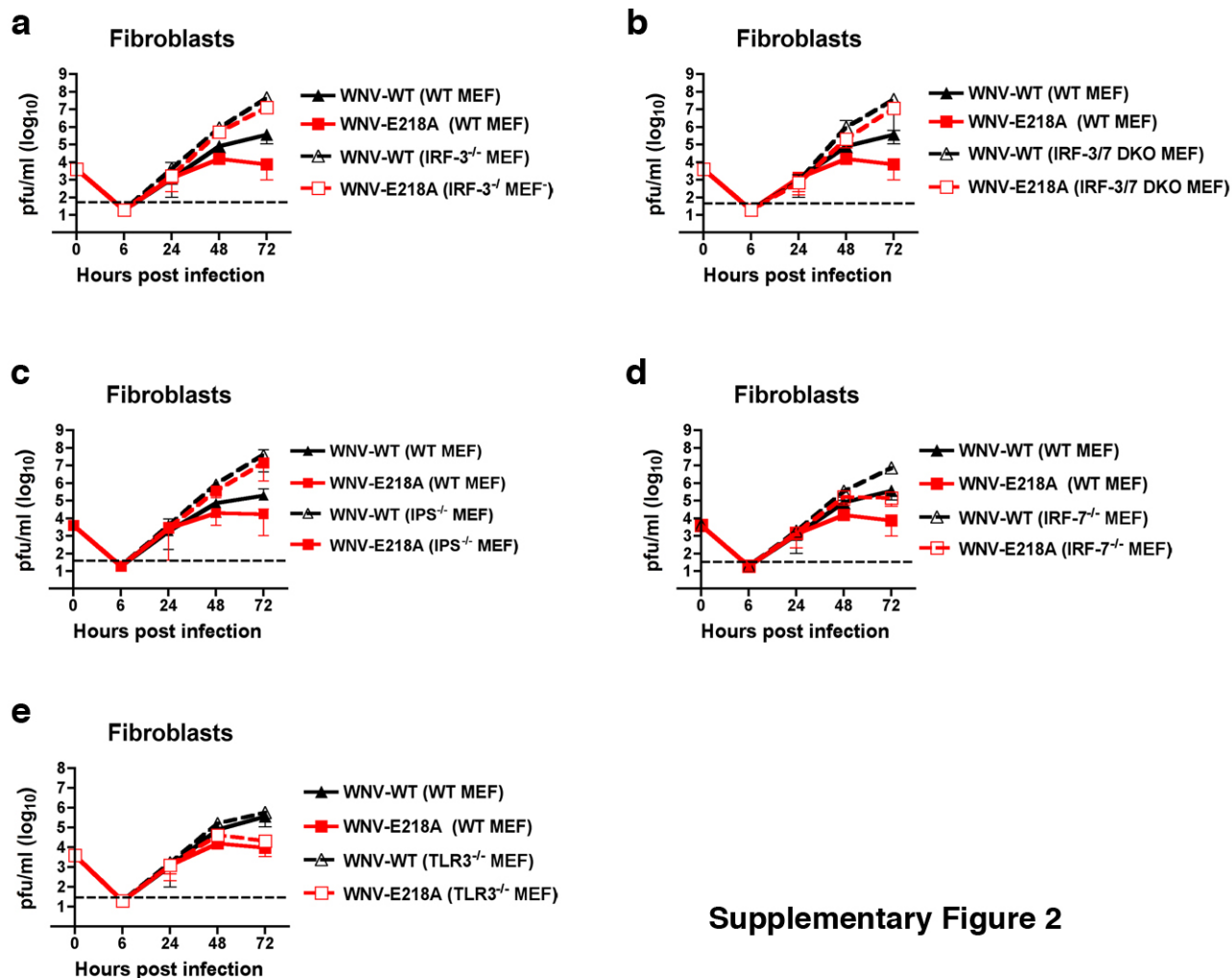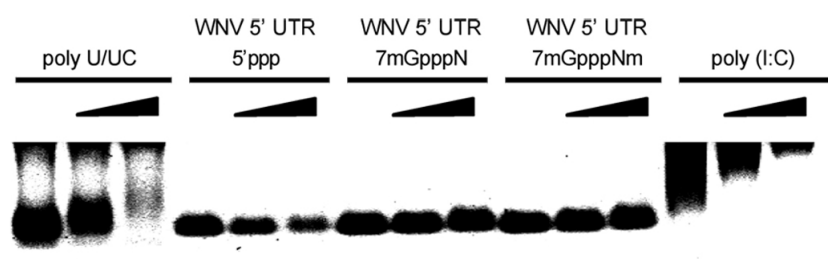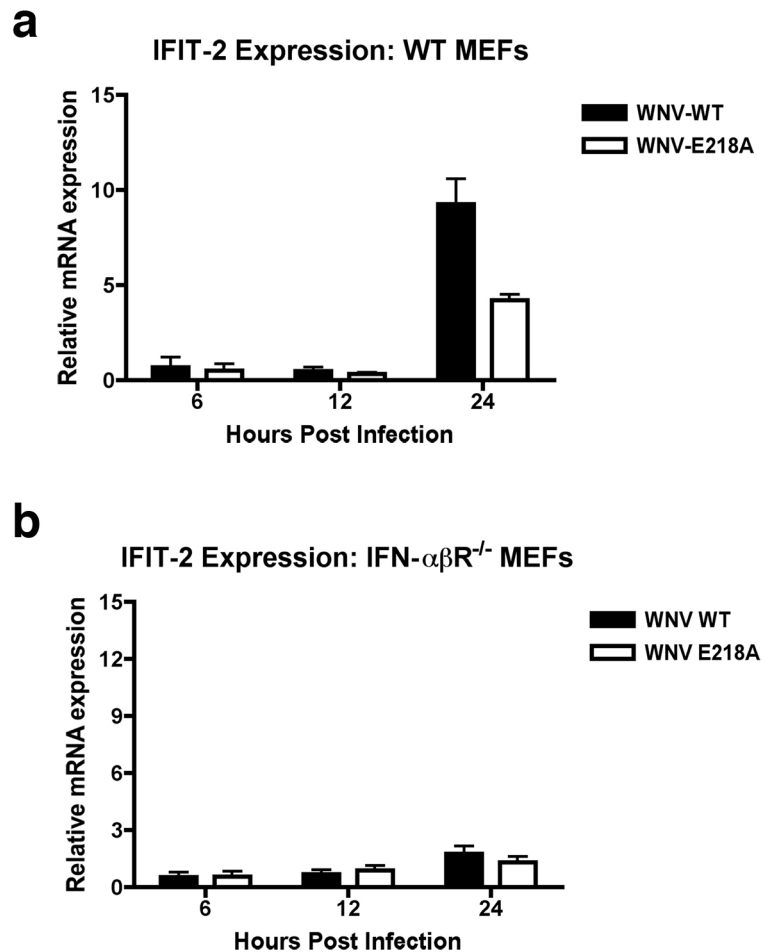
Supplementary Figure 2

Supplementary Figure 2. Replication of WNV-E218A is rescued in the *IRF-3$^{-/-}$*, *IRF-3$^{-/-}$* x *IRF-7$^{-/-}$* or *IPS-1$^{-/-}$* MEF. MEF generated from (**a-e**) wild type, (**a**) *IRF-3$^{-/-}$*, (**b**) *IRF-3$^{-/-}$* x *IRF-7$^{-/-}$*, (**c**) *IPS-1$^{-/-}$*, (**d**) *IRF-7$^{-/-}$*, or (**e**) *TLR3$^{-/-}$* mice were infected with WNV-WT or WNV-E218A at an MOI of 0.01 and virus production was evaluated at the indicated times post infection by plaque assay. Values are an average of quadruplicate samples generated from at least three independent experiments. Error bars indicate standard deviations. Differences in viral yield that are statistically significant are described in the text. Note, for direct comparison the growth curves for wild type MEFs are the same as shown in **Fig 1e**.
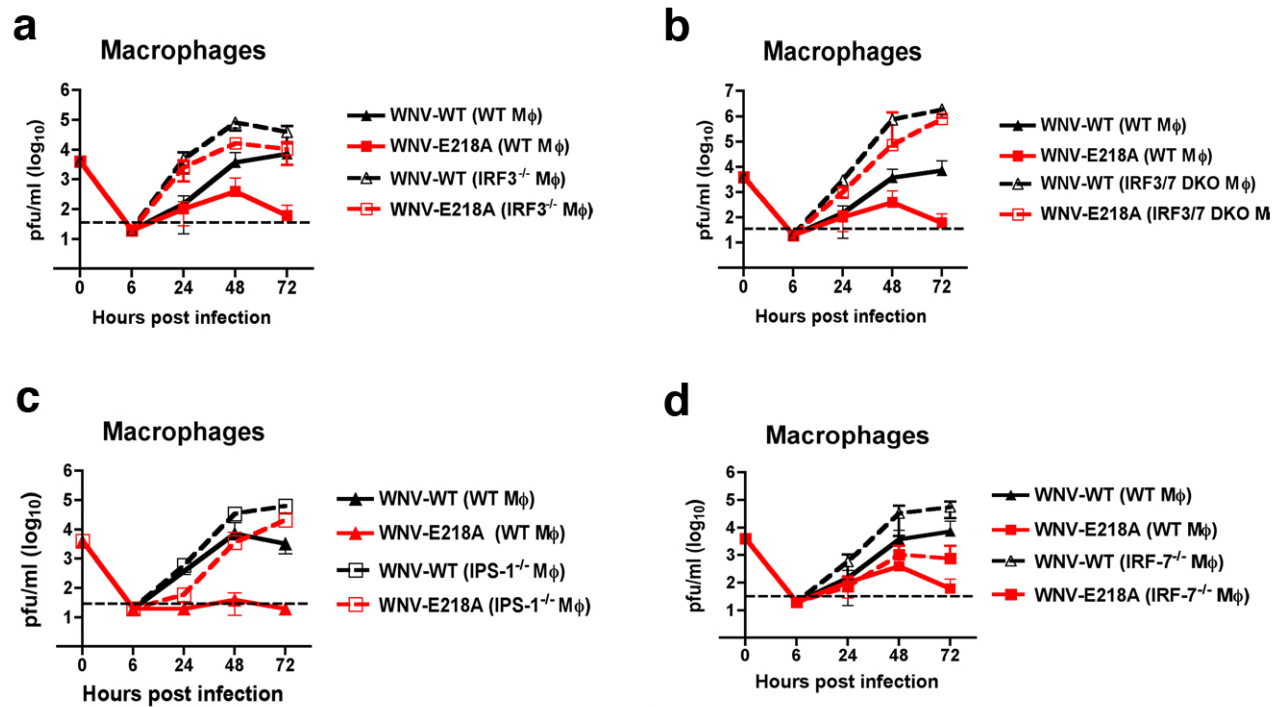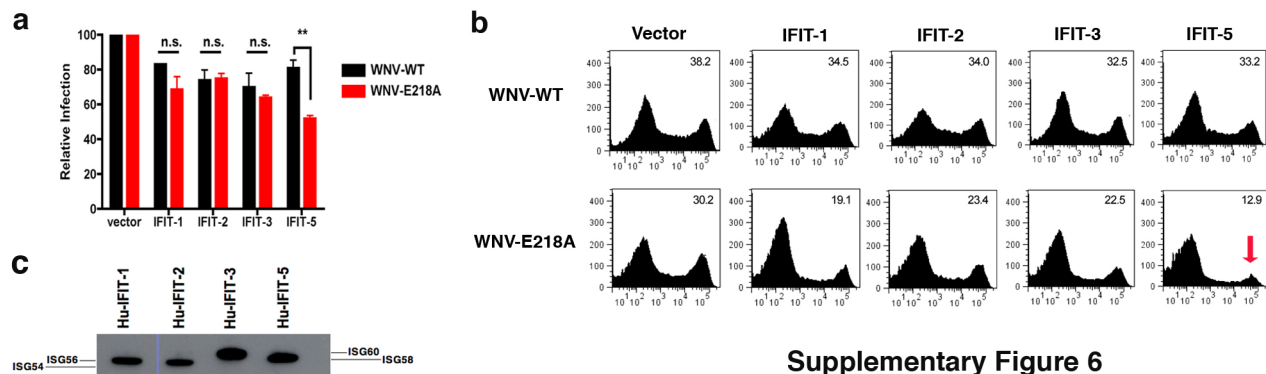
Supplementary Figure 3. Replication of WNV-E218A is rescued in the *IRF-3^{-/-}*, *IRF-3^{-/-}* x *IRF-7^{-/-}* or *IPS-1^{-/-}* Mϕ. Mϕ generated from (**a-d**) wild type, (**a**) *IRF-3^{-/-}*, (**b**) *IRF-3^{-/-}* x *IRF-7^{-/-}* (**c**) *IPS-1^{-/-}*, or (**d**) *IRF-7^{-/-}* mice were infected with WNV-WT or WNV-E218A at an MOI of 0.01 and virus production was evaluated at the indicated times post infection by plaque assay. Values are an average of quadruplicate samples generated from at least three independent experiments. Error bars indicate standard deviations. Differences in viral yield that are statistically significant are described in the text.

Supplementary Figure 4. RNA binding/gel-shift analysis of purified RIG-I with HCV poly-U/UC with a 5'ppp, WNV 5'UTR RNA with a 5'ppp, 7mGpppN (Cap 0), or 7mGpppNm (Cap 1) structure, and poly (I:C). Purified RIG-I (0, 15, and 60 pmol) was incubated with 6 pmol of the respective RNA. RIG-I efficiently bound to HCV poly U/UC and poly (I:C) and weakly to the WNV 5'UTR with a 5'ppp. Addition of a 2'O methyl group to the Cap 0 structure did not change RIG-I binding to the WNV 5'UTR RNA.

a

IFIT-2 Expression: WT MEFs

b

IFIT-2 Expression: IFN-$\alpha\beta$R$^{-/-}$ MEFs

Supplementary Figure 5. Expression of murine IFIT-2 in MEFs after WNV infection. (**a**) WT and (**b**) IFN-$\alpha\beta$R$^{-/-}$ MEFs were infected with WNV-WT or WNV-E218A (MOI of 1). At the indicated time points cells were harvested, mRNA was isolated, and levels of IFIT-2 mRNA were quantitated using TaqMan primers and probes after normalizing to levels of 18S ribosomal RNA. The data reflects the average of three experiments and the error bars indicate standard deviations.
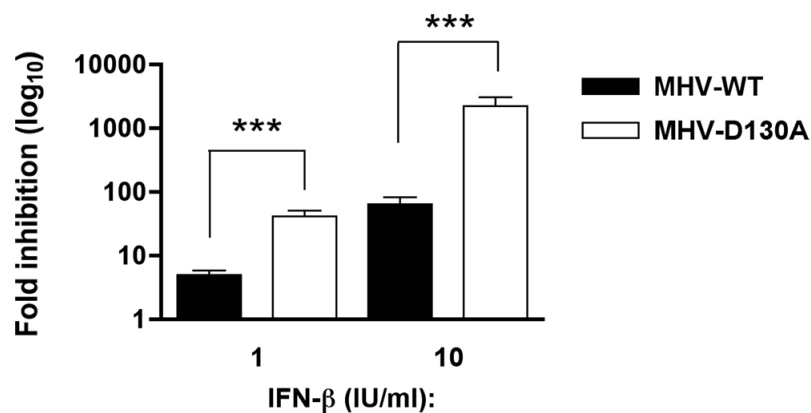
Supplementary Figure 6

Supplementary Figure 6. Transgenic expression of human IFIT-5 (Hu-IFIT-5) inhibits infection of WNV-E218A in 293T cells. Human 293T embryonic kidney cells were transfected transiently with vector alone, Hu-IFIT-1 (ISG56), Hu-IFIT-2 (ISG54), Hu-IFIT-3 (ISG60), or Hu-IFIT-5 (ISG58). Two days later, cells were infected with WNV-WT or WNV-E218A, and 24 hours later cells were processed for relative infection by flow cytometry using a MAb against WNV E protein. **a**. Summary of the effect of individual Hu-IFIT genes on WNV-WT or WNV-E218A. Infectivity as judged by flow cytometry (**b**) was normalized to the vector only plasmid. Data is the average of three independent experiments performed in triplicate. As the transfection efficiency was ~50%, (judged by parallel experiments with a GFP expression plasmid (data not shown)), the maximum expected reduction in infectivity for any of the human IFIT transgenes was 50%, this explaining the only partial inhibitory effect. **b**. Representative histograms of transfected cells infected with WNV-WT or WNV-E218A. The absolute percentage of WNV-infected cells is indicated in the top right corner of each histogram. The red arrow shows an example of selective inhibition of WNV-E218A by Hu-IFIT-5. **c**. Western blot of different Hu-IFIT genes after transient transfection of 293T cells. Note, each Hu-IFIT
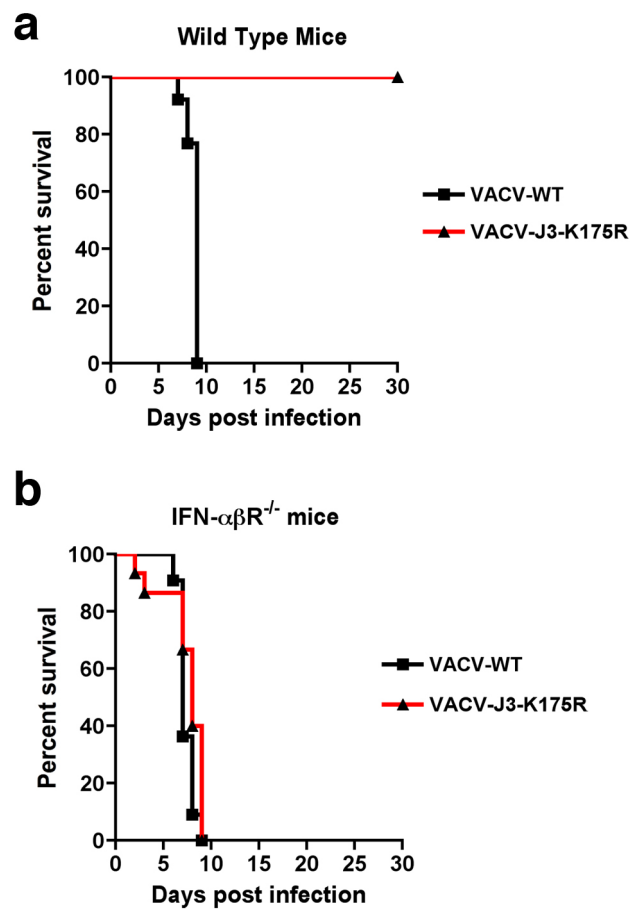
Supplementary Figure 7. VACV is attenuated in wild type mice but is virulent in *IFNαβR^{-/-}* mice. Survival curves of (**a**) wild type and (**b**) *IFNαβR^{-/-}* congenic C57BL/6 mice after intranasal infection of VACV-WT or VACV-J3-K175R. The survival difference between the wild type and mutant VAVC in wild type mice was statistically different (P = 0.002) whereas that in *IFNαβR^{-/-}* mice was not (P > 0.1). The deaths at day 2 and 3 following intranasal infection of two of the 15 *IFNαβR^{-/-}* mice with VACV-J3-K175R were outside of the median day of death. The significance of this early time of death is not known at present.

Supplementary Figure 8. 2'O methylation of viral RNA alters the sensitivity of MHV to the antiviral effects of IFN-β. IPS-1^{-/-} MEFs were pretreated with 1 or 10 IU/ml of IFN-β for 24 h prior to infection with MHV-WT and MHV-D130A. At 12 h after infection, supernatants were harvested, and viral burden was titrated by plaque assay. The data are the average of three independent experiments performed in triplicate, and the asterisks indicate differences that are statistically significant (***, $P < 0.0001$, **, $P < 0.005$, *, $P < 0.05$). Error bars indicate standard deviations.

REFERENCES

1   Ray, D. *et al*. West Nile virus 5'-cap structure is formed by sequential guanine N-7 and ribose 2'-O methylations by nonstructural protein 5. *J Virol* **80**, 8362-8370 (2006).

SUPPLEMENTARY METHODS

Generation of recombinant MHV-D130A

To generate the recombinant MHV-D130A a reverse genetic system established for MHV-A59 was used [1]. The full-length cDNA encoding for recombinant MHV-A59 was cloned into the vaccinia virus vNotI/tk and the corresponding recombinant vaccinia virus, designated vMHV-inf-1, was modified by two rounds of vaccinia virus-mediated homologous recombination using the *E.coli* guanosin-phosphoribosyltransferase (gpt) as a selection marker [2]. Initially, vMHV-inf-1 was recombined with plasmid pGPT-nsp16 (based on the plasmid pGPT-1 [3]) that contains the MHV nucleotides (nts) 20313-20816, the gpt gene, and MHV nts 21773-22274. The resulting recombinant vaccinia virus vMHV-gpt-nsp16, encoding for the MHV-A59 cDNA with the nsp16-encoding region replaced by the gpt gene, was obtained afer three rounds of plaque purification under gpt-positive selection [2]. The second recombination was performed with vMHV-gpt-nsp16 and the plasmid pD130A that encodes MHV nts 20665-21925 with the nucleotide substitution GAT to GCA at positions 21234 to 21236 to modify the active site (D130A) [4] of the MHV-A59 2'O-MT. The resulting recombinant vaccinia virus vMHV-D130A also was obtained after three rounds of plaque purification under gpt-negative selection. To generate the recombinant MHV-D130A, the vaccinia virus vMHV-D130A genomic DNA was purified, cleaved with the restriction enzyme EagI, and used for an T7-RNA polymerase-mediated in vitro transcription reaction. The resulting RNA was transfected into BHK-N cells [2] and produced recombinant MHV-D130A in the cell culture supernatant. The identity of MHV-D130A was confirmed by RT-PCR of viral RNA and sequencing analysis.

Gel-shift assays. Gel-shift assays were performed as previously described [5]. Briefly, 0 to 60 pmol of purified RIG-I was incubated with 6 pmol of RNA for 15 min at 37°C. RIG-I/RNA complexes were resolved on an agarose gel stained with SYBR© Gold (Invitrogen) and

formation of stable complexes was visualized by a shift/disappearance of RNA from its original migration pattern. HCV poly U/UC was prepared as previously described [5]. Poly (I:C) was obtained commercially (Sigma). The first 190 nucleotides of the WNV 5'UTR RNA were transcribed in vitro as previously described [6]. Following phenol/chloroform extraction and ethanol precipitation, WNV RNA was generated with a 5'ppp or Cap 0 or Cap 1 structure using kits (Epicentre Biotechnologies) according to the manufacturer's instructions.

SUPPLEMENTARY REFERENCES

1. Coley, S.E.*, et al*. Recombinant mouse hepatitis virus strain A59 from cloned, full-length cDNA replicates to high titers in vitro and is fully pathogenic in vivo. *Journal of virology* **79**, 3097-3106 (2005).
2. Eriksson, K.K., Makia, D. & Thiel, V. Generation of recombinant coronaviruses using vaccinia virus as the cloning vector and stable cell lines containing coronaviral replicon RNAs. *Methods in molecular biology (Clifton, N.J* **454**, 237-254 (2008).
3. Hertzig, T.*, et al*. Rapid identification of coronavirus replicase inhibitors using a selectable replicon RNA. *The Journal of general virology* **85**, 1717-1725 (2004).
4. Decroly, E.*, et al*. Coronavirus nonstructural protein 16 is a cap-0 binding enzyme possessing (nucleoside-2'O)-methyltransferase activity. *Journal of virology* **82**, 8071-8084 (2008).
5. Saito, T., Owen, D.M., Jiang, F., Marcotrigiano, J. & Gale, M., Jr. Innate immunity induced by composition-dependent RIG-I recognition of hepatitis C virus RNA. *Nature* **454**, 523-527 (2008).
6. Dong, H.*, et al*. West Nile virus methyltransferase catalyzes two methylations of the viral RNA cap through a substrate-repositioning mechanism. *Journal of virology* **82**, 4295-4307 (2008).